Journal of Computational Methods in Molecular Design, 2015, 5 (4):142-146

Scholars Research Library
(http://scholarsresearchlibrary.com/archive.html)

ISSN : 2231- 3176
CODEN (USA): JCMMDA

Quantum chemical origin of high ionization potential and low electron affinity of Tungsten Hexafluoride

Ambrish Kumar Srivastava[1], Anoop Kumar Pandey[2] and Neeraj Misra[1*]

[1]*Department of Physics, University of Lucknow, Lucknow, Uttar Pradesh, India*
[2]*Department of Physics, Govt. D. P. G. College, Dantewada, Chhattisgarh, India*

ABSTRACT

This paper deals with quantum chemical explanation of high ionization potential and low electron affinity of WF_6 as compared other species of this family. Calculated structure and vibrational frequencies of WF_6 by B3LYP, B3PW91 and MP2 schemes are compared with experimental values which establish superiority of B3PW91 over B3LYP and MP2 in the present case. Anionic and cationic forms of WF_6 are optimized and analysed at B3PW91 level. It is revealed that low electron affinity of WF_6 is due to extra electron localization on W which goes to antibonding molecular orbital. It is also shown that highest occupied molecular orbital is delocalized over F atoms and it is not easy to extract electron from electronegative F which results in very high ionization potential of WF_6.

Keywords: Tungsten hexafluoride, Electron affinity, Ionization Potential, Molecular Orbital, Atomic charge distribution.

INTRODUCTION

In the periodic table, transition metal elements have a great importance due to their variable coordination number. They form a variety of compounds which are referred to as coordination complexes. The nature of bonding in coordination complexes may vary depending upon the nature of its components, nature of metal and their oxidation states and ligands. Transition metal hexafluorides constitute an important class of coordination compounds which are well known for their distinguished structural and electronic properties. In such complexes, a central metal element is surrounded by six F ligands. The most common feature of hexafluorides includes an octahedral structure with high electron affinity (EA). However, octahedral symmetry may be broken due to an effect, so called, Jahn-Teller distortion, the high electron affinity of such species still gets attention of a wide community. Many transition metals have been reported to form hexafluoride molecules possessing very high electron affinities as compared to fluorine, at least, theoretically [1-7]. For instance, we have reported a systematic study on Osmium (Os) with a number of F ligands and found that OsF_6 is distorted to square planar (D_{4h}) geometry with adiabatic EA of about 6.5 eV [8]. Recently, our study [9] on WF_n (n = 1−5) species indicate that the tungsten fluorides behave differently than other transition metal fluorides.

Tungsten hexafluoride (WF_6) is well known for its distinguished properties. WF_6 is widely employed in the manufacture of semiconductor devices. It is used for deposition of tungsten metal to form interconnects due to its high conductivity and compatibility with the silicon substrate. In contrast to other hexafluorides of the same series, it is perfect octahedron. Moreover, it possesses very low electron affinity and very high ionization potential [1]. This is indeed a strong indication of its enormous stability against addition or removal of an electron from WF_6. In the present work, we perform a quantum chemical survey on these distinguished electronic properties of WF_6. We have tested various methods (B3LYP, B3PW91 and MP2) in order to choose appropriate scheme for the problem under study. To benchmark our calculations, we have compared calculated geometry and vibrational frequencies of WF_6 with corresponding experimental values. Finally, using atomic charge distribution and molecular orbital analysis at

the most appropriate level of theory, we have explained the origin of high ionization potential and low electron affinity of WF_6.

COMPUTATIONAL DETAILS

All computations were carried out with Gaussian 09 program [10] within ab initio density functional schemes. The functionals, in which Becke's three parameter exchange term (B3) [11] is combined with correlation terms of Lee, Yang and Parr (LYP) [12] as well as of Perdew and Wang (PW91) [13], were used. In addition, we have applied second order perturbation method of Moller and Plesset (MP2) [14]. All atom basis set of Stuttgart-Dresden-Dunning (SDD) was employed throughout these calculations. The visual animations of vibrational modes and all relevant graphics were generated with the help of GaussView 5 [15] and Chemcraft 1.8 packages [16].

RESULTS AND DISCUSSION

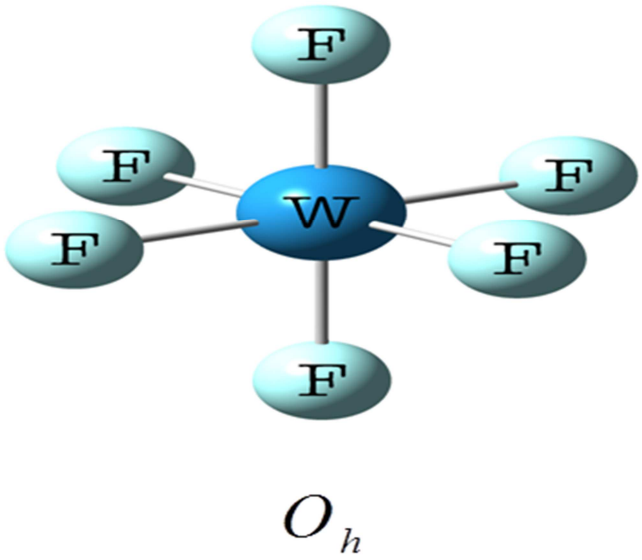

Figure 1. Model structure of Tungsten hexafluoride (WF_6)

Molecular structure and vibrations

The molecular structure of WF_6 is optimized by B3LYP, B3PW91 and MP2(FC) methods using SDD basis set. All methods lead to an octahedral (O_h) structure of WF_6 with singlet spin state as shown in Fig. 1. The calculated bond-lengths are 1.884, 1.878 and 1.903 A^o by B3LYP, B3PW91 and MP2 methods, respectively. The corresponding experimental value is 1.833 A^o measured by electron diffraction method [17]. Thus, B3PW91 calculated bond-length is more close to experimental value and highly overestimated by MP2 scheme.

Vibrational frequency calculations are also performed at the same level of theories within the harmonic approximation. Calculated harmonic frequencies and intensities are listed in Table 1. For a comparison, corresponding experimental values [18] are also included. The transition corresponding to symmetric stretching (a_{1g}) is calculated at 716 cm^{-1} by B3LYP, 722 cm^{-1} by B3PW91 and 699 cm^{-1} by MP2 against experimental value of 771 cm^{-1}. Very strong mode (t_{1u}) observed at 712 cm^{-1} is triply degenerate due to asymmetric stretching along three axes. A doubly degenerate mode (e_g) observed at 677 cm^{-1} also corresponds to asymmetric stretching, but along two planes.

Table 1. Vibrational modes of WF_6 calculated at B3LYP, B3PW91 and MP2 level with SDD basis set. Experimental values are also included for comparison

Modes	B3LYP		B3PW91		MP2		Experiment[c]	
	Freq.[a]	Intensity[b]	Freq.	Intensity	Freq.	Intensity	Freq.	Intensity
a_{1g}	716	0.0	722	0.0	699	0.0	771	inactive
t_1u	695	222.6	700	226.7	682	260.7	712	v. strong
e_g	645	0.0	651	0.0	629	0.0	677	inactive
t_2g	288	0.0	291	0.0	291	0.0	320	inactive
t_1u	223	39.7	225	39.4	231	39.3	258	strong
t_2u	115	0.0	116	0.0	123	0.0	127	inactive

[a]Frequency in cm^{-1}; [b]Intensity in a.u.; [c]Ref. [18].

All other lower modes associated with bending and distortions are triply degenerate due to symmetry of vibrations. Also due to highly symmetric structure of WF_6, most of IR modes become inactive. From Table 1, one can see that for a_{1g}, e_g, t_{2g} and t_{2u} modes, IR intensities vanish. In general, our computational methods reproduce and assign experimental bands correctly. The differences between calculated and observed frequencies are mainly due to anharmonicity of vibrations, which go on decreasing for lower frequencies for all three methods employed. It should be noticed, however, that B3PW91 calculated frequencies are more close to experimental values as compared to B3LYP and MP2.

Ionization potential and electron affinity

In order to discuss the effect of addition and removal of an electron, we have optimized the structures of anionic and cationic WF_6 at B3PW91 level of theory. The equilibrium geometries of WF_6^- and WF_6^+ are displayed along with neutral WF_6 in Fig. 2. Evidently, addition of an electron does not affect the molecular geometry of WF_6. It results only in a marginal increase in the bond-length (by 0.01 A^o). On the other hand, removal of an electron leads to change the structure into complex form, $(WF_4)F_2$. In this complex, two F atoms go away from the central W forming a F_2 moiety with the distance of 1.935 A^o. The distance of this moiety from centre is increased to 2.302 A^o, whereas other bond-lengths are decreased to 1.843-1.851 A^o.

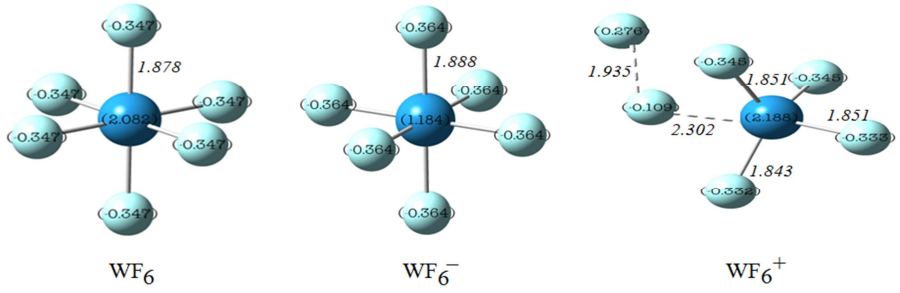

Figure 2. Equilibrium geometries of WF_6, WF_6^- and WF_6^+ at B3PW91/SDD level. Atoms are labeled with NBO charges (in e) and bond-lengths (in A^o) are also shown

We discuss the origin of high ionization potential and low electron affinity of WF_6. We analyze the distribution of extra electron over W and F atoms referring to charges labeled on atoms in Fig. 2. These atomic charges are calculated by natural bonding orbital (NBO) analysis [19,20] which are more reliable due to their less basis set dependency. In neutral WF_6, atomic charge on W is +2.08 e and -0.35 e is contained by each F atom. First we consider the case of removal of an electron, i.e. WF_6^+. The ionization potential (IP) of WF_6 is calculated to be about 15 eV which is consistent with the experimental value of 15.24 ± 0.10 eV by Hildenbrand [21]. In order to explain such a high IP, we examine the charge distribution upon ionization of WF_6. The electron is mainly contributed by 2p atomic orbital of two F atoms which forms a F_2 moiety. W atom contributes only 0.1 e during the process of ionization which results in very high IP of WF_6.

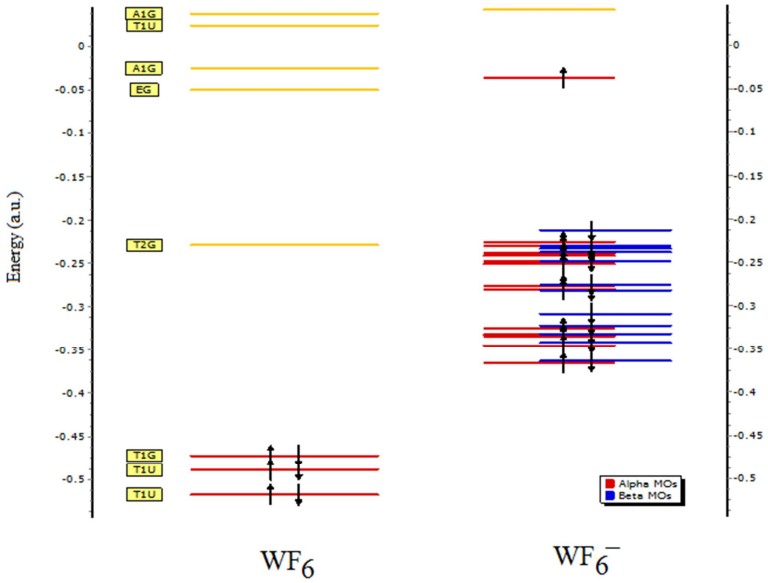

Figure 3. Molecular orbital diagrams of WF_6 and WF_6^- at B3PW91/SDD level

Similarly, the EA of WF_6 has been estimated as 3.9 eV which is slightly higher than experimentally estimation of 3.4 - 3.7 eV [22-24]. However, note that this value is very small as compared to those of other hexafluorides of 5d series. For instance, the EA of PtF_6, 6.85 eV [25] is almost two times that of WF_6. In general, large EA of hexafluorides results due to extra electron delocalization over several F atoms, leaving electron deficiency at the centre. But this is not the case for WF_6 in which extra electron is completely localized on W atom. The NBO charge difference on W in WF_6 and WF_6^- is 0.9 e (see Fig. 2). Thus 90% of extra electron is located on W and only 10% is shared equally by peripheral F atoms. The extra electron localization on W disables it to be electron deficient, consequently lowering the EA of WF_6.

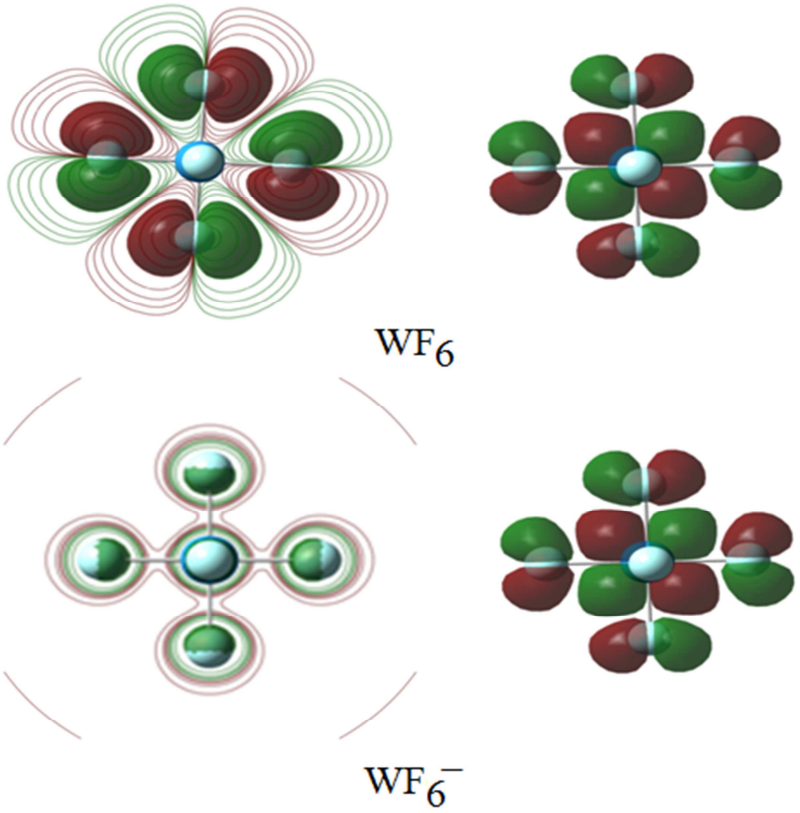

Figure 4. HOMO (left) and LUMO (right) plots of WF_6 and WF_6^- calculated at B3PW91/SDD level

Let us now discuss these electronic properties from molecular orbital (MO) perspectives. W possesses an outer shell configuration of $5d^4 6s^2$. Due to sextet ($5d^5 6s^1$) configuration as its ground state, it can easily bind with six F ($2s^2 2p^4$) atoms. In WF_6, due to the interaction of d orbitals of W and p orbitals of F, d energy levels split into two sets. First set e_{1g} ($d_{x^2-y^2}$, d_{z^2}) is 0.64 eV above the second t_{1g} (d_{xy}, d_{yz}, d_{xz}). The MOs are constructed from metal and ligand orbitals symmetry as shown in Fig. 3 for WF_6 and WF_6^-. We focus on frontier MOs as they are mainly responsible for chemical reactions or interactions. The highest occupied molecular orbital (HOMO) represents ability to donate an electron while lowest unoccupied molecular orbital (LUMO) denotes ability to accept it. The energy gap between HOMO and LUMO can be used as a stability index of molecule. Figure 4 displays the HOMO-LUMO surfaces for WF_6 and WF_6^-. Apparently, the HOMO of WF_6 is delocalized over F atoms i.e. ligand MO. Due to strong electronegative nature of F atoms, it is not favorable to extract an electron which is the reason behind high IP of WF_6.

Addition of an electron to WF_6 causes to shift e_{1g} and t_{1g} levels increasing their separation to 0.78 eV, consequently, increasing the energies of HOMO and LUMO. This extra electron goes to antibonding MO of WF_6 as shown in Fig. 3 and in the HOMO plot of WF_6^- as well (see Fig. 4). This causes to slightly destabilize the molecule due to repulsion created by antibonding electron which is reflected by decrease in HOMO-LUMO gap of WF_6 by addition of an electron. Note the HOMO-LUMO gaps of WF_6 and WF_6^- are 6.53 eV and 2.18 eV, respectively. This also explains the low EA value of WF_6.

CONCLUSION

In summary, we have used B3PW91 method to explain the high ionization potential and low electron affinity of WF_6. The reliability of B3PW91 over B3LYP and MP2 is established by calculating structure and vibrational

frequencies of WF_6. We have shown that low electron affinity of WF_6 is due to extra electron localization on W and highest occupied molecular orbital is delocalized over F atoms which results in very high ionization potential of WF_6. Thus present study provides a theoretical explanation of distinguished electronic properties of tungsten hexafluoride.

Acknowledgement
AKS acknowledges Council of Scientific and Industrial Research (CSIR), New Delhi, India for a research fellowship.

CONFLICT OF INTEREST
The authors declare that there is no conflict of interests regarding the publication of this paper. Also, they declare that this paper or part of it has not been published elsewhere.

CONTRIBUTION OF THE AUTHORS
AKS performed all calculations and prepared the draft. AKP contributed in writing the paper. NM designed the research and finalized the draft. AKS, AKP and NM revised the draft paper. All authors read and approved the final version.

REFERENCES

[1] GL Gutsev; AI Boldyrev, *Chem. Phys. Lett.*, **1983**, 101, 255-258.
[2] AK Srivastava; SK Pandey; N Misra, *Chem. Phys. Lett.*, **2015**, 624, 15-18.
[3] J Yang; XB Wang; XP Xing; LS Wang, *J. Chem. Phys.*, **2008**, 128, 201102.
[4] AK Srivastava; N Misra, *J. Comput. Methods Mol. Des.*, **2014**, 4, 63-67.
[5] AK Srivastava; N Misra, *Mol. Phys.*, **2015**, 113, 36-44.
[6] SA Siddiqui; AK Pandey; T Rasheed; M Mishra, *J. Fluorine Chem.*, **2012**, 135, 285-291.
[7] AK Pandey; AK Srivastava; A Dwivedi, *Main Group Chem.*, **2015**, 14, 291-299.
[8] AK Srivastava; N Misra, *J. Fluorine Chem.*, **2014**, 158, 65-68.
[9] AK Srivastava; AK Pandey; N Misra, *J. Chem. Sci.*, **2015**, 127, 1853-1858.
[10] MJ Frisch; GW Trucks; HB Schlegel; GE Scuseria; MA Robb, et al., Gaussian 09, Rev. B.01, Gaussian, Inc. Wallingford, CT, **2010**.
[11] AD Becke, *J. Chem. Phys.*, **1993**, 98, 5648-5652.
[12] C Lee; W Yang; RG Parr, *Phys. Rev. B*, **1988**, 37, 785-789.
[13] JP Perdew; Y Wang, *Phys. Rev. B*, **1992**, 45, 13244-13249.
[14] C Moller; MS Plesset, *Phys. Rev.*, **1934**, 46, 618-622.
[15] R Dennington; T Keith; J Millam, GaussView 5.0, Semichem Inc. Shawnee, KS, **2005**.
[16] GA Zhurko; DA Zhurko, Chemcraft version 1.8, **2012**. www.chemcraftprog.com.
[17] M Hargittai, *Chem. Rev.*, **2000**, 100, 2233-2301.
[18] T Shimanouchi, Tables of Molecular Vibrational Frequencies Consolidated Volume I, National Bureau of Standards, **1972**, 1-160.
[19] AE Reed; RB Weinstock; F Weinhold, *J. Chem. Phys.*, **1985**, 83, 735-746.
[20] ED Glendening; JK Badenhoop; AE Reed; JE Carpenter; F Weinhold, NBO. 3.1 Program, Theoretical Chemistry Institute, University of Wisconsin. Madison,WI, **1996**.
[21] DL Hildenbrand, *J. Chem. Phys.*, **1975**, 62, 3074.
[22] PM George; JL Beauchamp, *Chem. Phys.*, **1979**, 36, 345-351.
[23] AA Viggiano; JF Paulson; F Dale; M Henchman; NG Adams; D Smith, *J. Phys. Chem.*, **1985**, 89, 2264-2267.
[24] H Dispert; K Lacmann, *Chem. Phys. Lett.*, **1977**, 45, 311-315.
[25] N Bartlett, *Proc. Chem. Soc. London*, **1962**, 6, 218.